

Broadband Radiative Flux and the Vertical Structure of Humidity and Temperature in the Atmosphere

T. L. Alberta
Analytical Services and Materials, Inc.
Hampton, Virginia

T. P. Charlock
NASA-Langley Research Center
Hampton, Virginia

Introduction

CAGEX [Cloud and Earth Radiant Energy System (CERES)/Atmospheric Radiation Measurement (ARM)/Global Energy and Water Experiment (GEWEX)] Version 2.1.0 provides five largely independent descriptions of the temperature and humidity fields over the ARM Southern Great Plains (SGP) Cloud and Radiation Testbed (CART) site for the September 25 to November 1, 1995, ARM Enhanced Shortwave Experiment (ARESE). Vertical profiles of shortwave (SW) and longwave (LW) fluxes have been computed with these soundings used as inputs for the Fu and Liou delta-four stream code as modified by Kratz and Rose (1998, personal communication). 1) The “Core” soundings for temperature and humidity are based on 3-hourly ARM radiosondes; 2) the “Eta” sounding profiles are based on the National Weather Service (NWS) Eta mesoscale model Data Assimilation System (EDAS), which used standard 12-hourly radiosondes; 3) the “atmospheric emitted radiance interferometer (AERI)” sounding modifies the Core soundings below 2 km with temperature and humidity retrievals from a Fourier Transform Spectrometer; 4) a fourth sounding “microwave radiometer (MWR)” uses precipitable water derived from the ARM MWR to scale humidity in (3); and 5) the “Global Positioning System (GPS)” sounding scales (1) with precipitable water derived from GPS.

Under clear skies, all humidity data sets produced quite accurate simulations of the direct component of the surface SW insolation. For mean top of the atmosphere (TOA) insolation over 700 W/m^2 , the computed direct was 11 W/m^2 to 17 W/m^2 (2% to 4%); no significant dependence of the SW direct error on H_2O or aerosol optical depth (AOD) path length was found. The computed diffuse component of SW exceeded measurements by 27 W/m^2 to 30 W/m^2 (43% to 50%), with weak indication of path length dependence. For LW, significant differences in individual

vertical profiles of humidity led to discrepancies in clear-sky cooling rates. This paper has two parts: a discussion of the vertical structure of temperature and humidity in CAGEX, and an examination of the clear-sky shortwave surface insolation bias (Charlock et al. 1998) and its dependence upon aerosol and water vapor path lengths.

Vertical Structure of the Atmosphere

CAGEX (Charlock and Alberta 1996) has made available five somewhat independent representations of vertical temperature and humidity profiles. Figure 1 depicts the column precipitable waters for the five profiles. All profiles

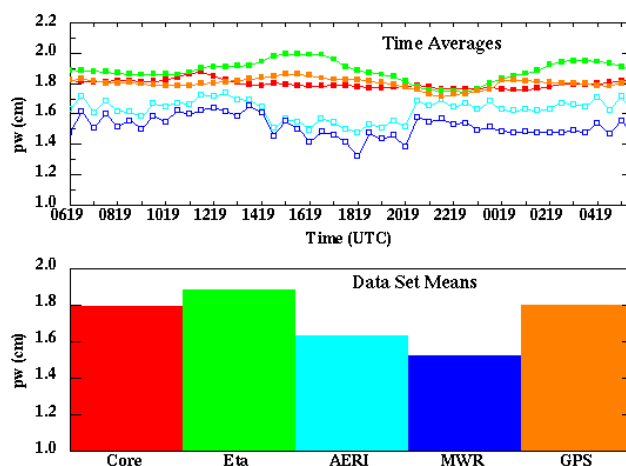


Figure 1. Precipitable water for the five CAGEX V2 profiles. AERI and MWR profiles are denoted by open circles in the time averages (top). (For a color version of the figure, please see http://www.arm.gov/docs/documents/technical/conf_9803/alberta-98.pdf.)

are within 0.4 cm of each other, with the AERI and MWR profiles being the driest. Time averages show this dryness occurring mostly during the daytime hours.

Figure 2 depicts the common-domain data set means of two CAGEX profiles: Core and Eta. Temperatures are similar except at low levels (below 850 hPa). Taken as a whole, the Eta profiles are 3° K or 4° K cooler at the surface. Eta is more moist above 650 hPa, and drier below. These differences have a significant effect on the heating rates in the troposphere, and also on the outgoing longwave radiation (OLR) (Table 1) calculated by the Fu-Liou code, using the two profiles as input. The heating rate profile calculated using Eta shows greater/lesser cooling above/below 500 hPa than that calculated using the core sounding profiles.

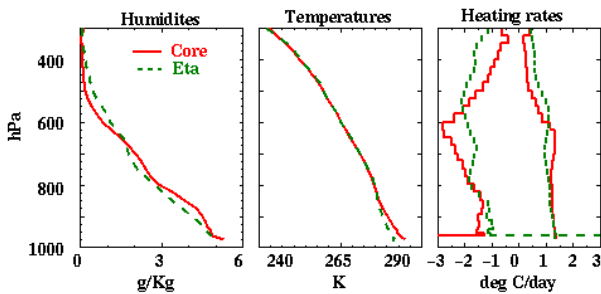


Figure 2. Data set-averaged mean profiles for Core (solid) and Eta (dashed) data sets. SW heating rates are represented by the lines furthest right on the heating rate plot. LW is to the left, negative heating denoting cooling. (For a color version of the figure, please see http://www.arm.gov/docs/documents/technical/conf_9803/alberta-98.pdf.)

Table 1. Selected flux biases for CAGEX V2.1, using the five CAGEX profiles as input to the radiative transfer code.

	Core	ETA	AERI	MWR	GPS
SFC* SW Direct	11	12	11	12	12
SFC* SW Diffuse	30	27	29	29	30
SFC* SW Insolation	40	39	40	41	42
TOA OLR	8	5	7	9	8

*SFC = surface

Although significant differences exist between the five sets of CAGEX V2 profiles, Table 1 clearly indicates that none of these profiles result in calculations of SW surface insulations, which agree with measurements.

Dependence of SW Surface Insolation Bias on Path Lengths

To examine a possible link between path length and the SW surface insolation bias found in CAGEX, we focused our attention on AOD and precipitable water from the core profiles (based upon ARM sondes) in clear sky. We defined path length as the optical depth or precipitable water divided by the cosine of the zenith angle. When examining measurements, we used separate, direct, and diffuse radiometry, and focused on transmission rather than insolation. Transmission is defined as surface flux (direct, diffuse, and total) divided by the TOA insolation. It should be noted here that because the magnitude of diffuse transmission is significantly smaller than that of direct, a 1% bias in diffuse transmission represents a larger error than that of direct.

Figure 3 shows the relationship between total flux (clear-sky) transmission bias and the AOD path length. The correlation coefficient calculated using this data is 0.67, indicating the possibility of a relationship between the two parameters. The transmission bias increases as the AOD path length increases. When plotting direct horizontal flux transmission bias against AOD (Figure 4), the relationship is not evident. It should be noted that the points shown on the plot, representing a bias of 0.05 and greater, disappear when using a stringent radiometer-based clear-sky mask (C. Long, 1998, personal communication). A marked transmission bias is seen with the diffuse transmission plotted against the AOD (Figure 5). Similar relationships can be seen when plotting these biases against precipitable water path length. Figure 6 is an example of this bias diffuse transmission.

Although these plots hint at a relationship between clear-sky transmission bias and path length, the data set is too small to make a definitive judgment. CAGEX version 2.2, which will be released soon, will have a somewhat larger data set due to the inclusion of a couple more days of Geostationary Operational Environmental Satellite (GOES) clouds.

The radiometer-based clear-sky mask will be applied to V2.2, and may clean up some cloud contamination, yielding more confident results. CAGEX V3 will soon begin, covering the August 1998 ARM Intensive Observation Period (IOP). That, in addition to CAGEX V1, should supply a large enough sample size to instill more confidence in these results.

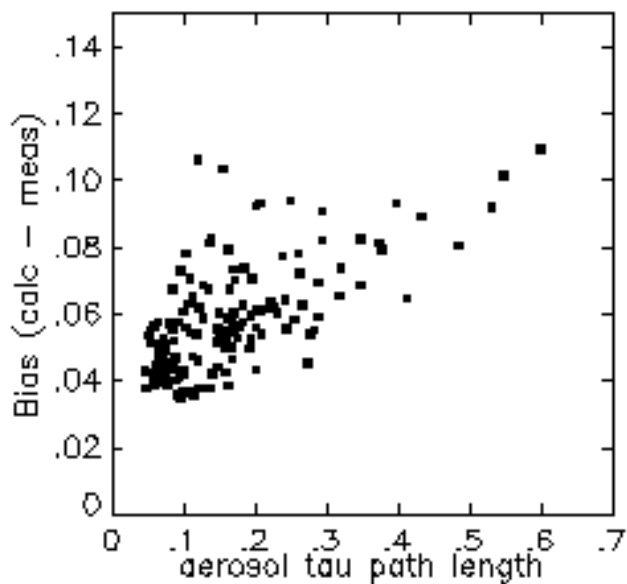


Figure 3. SW clear-sky biases. Transmission of total insolation as a function of AOD path length.

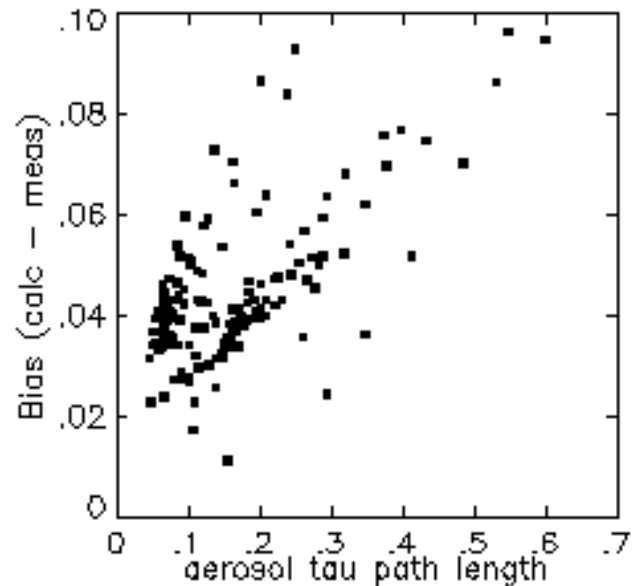


Figure 5. Same as Figure 3, except diffuse transmission biases are plotted.

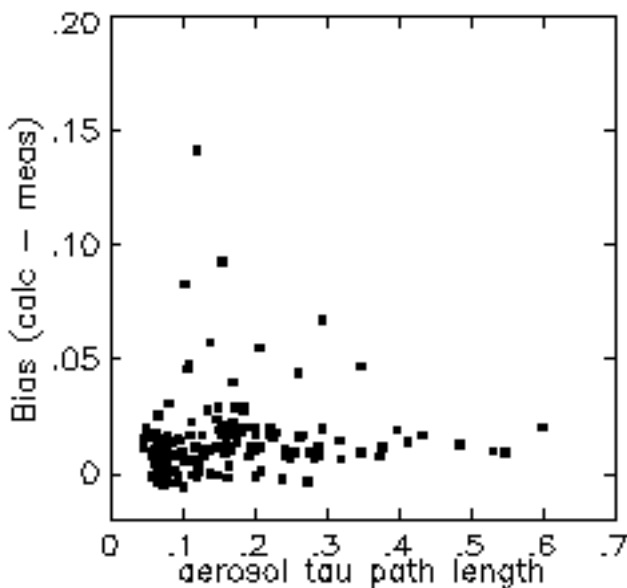


Figure 4. Same as Figure 3, except direct horizontal biases are plotted.

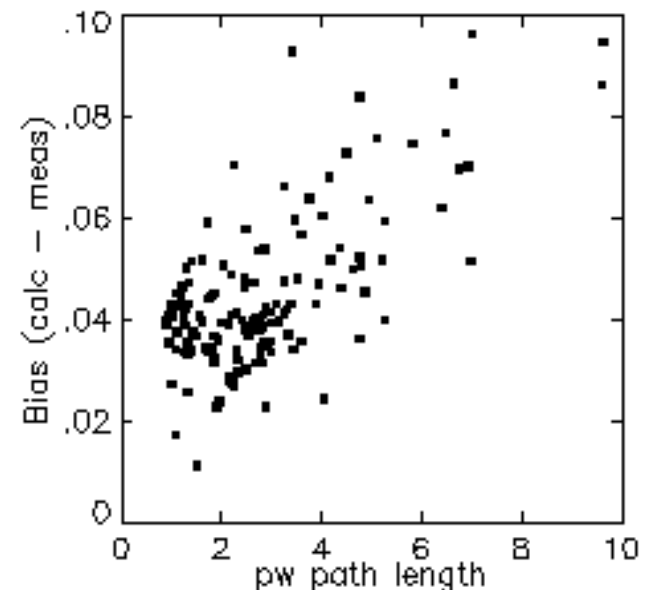


Figure 6. Same as Figure 5, except biases are plotted against precipitable water path length.

References

Charlock, T. P., and T. L. Alberta, 1996: The CERES/ARM/GEWEX Experiment (CAGEX) for the retrieval of radiative fluxes with satellite data. *Bull. Amer. Meteor. Soc.*, **77**, 2673-2683.

Charlock, T. P., F. G. Rose, T. L. Alberta, and G. D. Considine, 1998: Comparison of computed and measured cloudy-sky shortwave (SW) in the ARM Enhanced Shortwave Experiment (ARESE). This proceedings.